© 2020. Published by The Company of Biologists Ltd | Journal of Cell Science (2020) 133, jcs240879. doi:10.1242/jcs.240879

RESEARCH ARTICLE

Sarcoplasmic reticulum Ca^{2+} decreases with age and correlates with the decline in muscle function in *Drosophila*

Alba Delrio-Lorenzo*, Jonathan Rojo-Ruiz*, María Teresa Alonso and Javier García-Sancho‡

ABSTRACT

Sarcopenia, the loss of muscle mass and strength associated with age, has been linked to impairment of the cytosolic Ca^{2+} peak that triggers muscle contraction, but mechanistic details remain unknown. Here we explore the hypothesis that a reduction in sarcoplasmic reticulum (SR) Ca^{2+} concentration ($[Ca^{2+}]_{SR}$) is at the origin of this loss of Ca^{2+} homeostasis. We engineered *Drosophila melanogaster* to express the Ca^{2+} indicator GAP3 targeted to muscle SR, and we developed a new method to calibrate the signal into $[Ca^{2+}]_{SR}$ *in vivo*. $[Ca^{2+}]_{SR}$ fell with age from ∼600 µM to 50 µM in close correlation with muscle function, which declined monotonically when $[Ca^{2+}]_{SR}$ was <400 µM. $[Ca^{2+}]_{SR}$ results from the pump-leak steady state at the SR membrane. However, changes in expression of the sarco/endoplasmic reticulum Ca^{2+}-ATPase (SERCA) pump and of the ryanodine receptor leak were too modest to explain the large changes seen in $[Ca^{2+}]_{SR}$. Instead, these changes are compatible with increased leakiness through the ryanodine receptor as the main determinant of the $[Ca^{2+}]_{SR}$ decline in aging muscle. In contrast, there were no changes in endoplasmic reticulum $[Ca^{2+}]$ with age in brain neurons.

This article has an associated First Person interview with the first author of the paper.

KEY WORDS: Aging, Calcium homeostasis, Calcium imaging, *Drosophila melanogaster*, Endoplasmic reticulum, Fly, SERCA, Sarcopenia, Sarcoplasmic reticulum, Ryanodine receptor

INTRODUCTION

Aging is characterized by a gradual loss of function of tissues and organs that ultimately leads to death (Marzetti and Leeuwenburgh, 2006). Skeletal muscle is one of the most severely affected tissues and as a result of aging, it loses mass and strength, which is known as sarcopenia (Vijg and Campisi, 2008). Age-dependent sarcopenia is not restricted to mammals, as it affects other animals, including nematodes and flies (Bass et al., 2007). Although much attention has been devoted to the mechanisms underlying sarcopenia and to putative treatments to reverse it, success has been limited. The dominant idea is that there is a deficiency in muscular excitation–contraction coupling due to loss of Ca^{2+} homeostasis.

Increases in cytosolic Ca^{2+} concentration ($[Ca^{2+}]_C$) are the trigger for cell activation in many different tissues (Berridge, 2016; Berridge et al., 2003). In mammalian skeletal muscle, the action potential at the sarcolemma spreads through the T-system and activates ryanodine receptor type 1 (RyR1) at the sarcoplasmic reticulum (SR). RyR1 has a built-in channel, the opening of which promotes large Ca^{2+} release from the SR, which transiently increases the $[Ca^{2+}]_C$, and triggers muscular contraction through the sliding of the myofilaments (Allen et al., 2008; Efremov et al., 2015; Zalk et al., 2007). Changes of Ca^{2+} binding inside SR can also contribute to determine the shape and the extent of the Ca^{2+} transient (Manno et al., 2017; Ríos, 2018; Sztretye et al., 2011a).

Changes in $[Ca^{2+}]_{SR}$ can be monitored either with synthetic Ca^{2+} indicators or with genetically encoded Ca^{2+} indicators. Although many members of the first group have revealed important properties of muscle activation (Kabbara and Allen, 2001; Launikonis et al., 2005, 2006; Ziman et al., 2010), genetically encoded Ca^{2+} indicators achieve higher organelle selectivity (Alonso et al., 2017; Canato et al., 2010; Manno et al., 2017; Ríos, 2018; Sztretye et al., 2011b). A decrease in $[Ca^{2+}]_{SR}$ has been reported in isolated mice skeletal fibers with the biosensor D1ER after application of 4-chloro-*m*-cresol or electrical stimulation (Jiménez-Moreno et al., 2010; Rudolf et al., 2006; Canato et al., 2010).

According to the 'calcium hypothesis', aging is related to dysregulation of Ca^{2+} homeostasis. This can include not only alterations in $[Ca^{2+}]_C$, but also in the Ca^{2+} concentration in the mitochondria and/or other cytoplasmic organelles (Alzheimer's Association Calcium Hypothesis Workgroup, 2017; Thibault et al., 2007). One of the most convincing theories postulates that RyR1 is subjected to progressive damage that increases the 'leakiness' of the SR to Ca^{2+}, leading to a reduction in $[Ca^{2+}]_{SR}$. This will result in a decline in the increased $[Ca^{2+}]_C$ transients and in the force produced, particularly for responses to high-frequency stimulation (70 Hz) that cause tetanic muscle stimulation (Andersson et al., 2011; Bellinger et al., 2009, 2008; Jiménez-Moreno et al., 2008, 2010). However, to date, no reliable measurements of $[Ca^{2+}]_{SR}$ have been reported for living animals of different ages.

Here we investigated the role of $[Ca^{2+}]_{SR}$ homeostasis during aging using a variant of the recently developed green fluorescent protein–aequorin protein (GAP) Ca^{2+} indicators. GAP can be targeted to the endoplasmic reticulum (ER), thus allowing direct and selective measurement of $[Ca^{2+}]_{ER}$ (Navas-Navarro et al., 2016; Alonso et al., 2017). We chose the *Drosophila melanogaster* model and generated transgenic flies for *in vivo* monitoring of $[Ca^{2+}]_{ER}$ in muscle and neurons (Alonso et al., 2017; Navas-Navarro et al., 2016; Rodriguez-Garcia et al., 2014).

We show that $[Ca^{2+}]_{SR}$ in muscle decreases progressively with age, and that this reduction closely correlates with muscle loss of function. The expression of sarco/endoplasmic reticulum Ca^{2+}-ATPase (SERCA) was decreased in the muscle of aged flies, although not enough to account for the much larger decrease in $[Ca^{2+}]_{SR}$. Our data support the view that age-related changes in SR leakiness are mainly responsible for this decrease in pump-leak steady state that results in

Instituto de Biología y Genética Molecular (IBGM), Universidad de Valladolid y Consejo Superior de Investigaciones Científicas (CSIC), c/Sanz y Forés 3, 47003 Valladolid, Spain.
*These authors contributed equally to this work

‡Author for correspondence (jgsancho@ibgm.uva.es)

J.G.-S., 0000-0003-4573-7930

Received 21 October 2019; Accepted 24 January 2020

Journal of Cell Science (2020) 133, jcs240879. doi:10.1242/jcs.240879

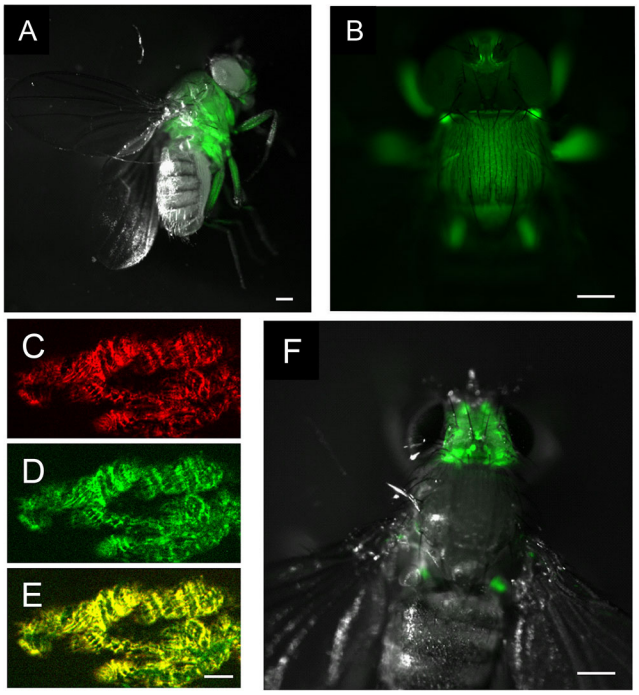

Fig. 1. Specific expression of erGAP3 in the thoracic muscle and brain neurons of *Drosophila melanogaster*. (A,B) Lateral (A) and dorsal (B) views of the thoracic muscles expressing erGAP3 in the *Mhc-erGAP3* fly line. The green fluorescence images (F_{470}) were superimposed on bright field images. (C–E) Confocal microscopy images of fly muscle fibers expressing erGAP3 (green in panel D) and immunostained for SERCA (red in panel C). The merged image shows the co-localization of both proteins (panel E). Note the striated pattern of the images. (F) Dorsal view of head neurons expressing erGAP3 in *elav-erGAP3* line. Scale bars: 200 µm (A,B,F); 5 µm (C–E).

the $[Ca^{2+}]_{SR}$ decline. In contrast to muscle, $[Ca^{2+}]_{ER}$ in brain neurons showed no significant changes with age, which indicates tissue selectivity for the loss of Ca^{2+} homeostasis during aging.

RESULTS

Transgenic flies expressing ER-targeted GAP3

To measure $[Ca^{2+}]_{ER}$, we generated transgenic flies that expressed ER-targeted GAP3 (erGAP3) in skeletal muscle (Navas-Navarro et al., 2016) or in neurons (see Materials and Methods). GAP3 is a low-affinity Ca^{2+} indicator (K_d=489 µM) that is suitable for measuring $[Ca^{2+}]$ between 0.05 and 2.0 mM. This $[Ca^{2+}]$ range covers the wide span of the ER/SR lumen concentrations previously reported for different tissues and under different conditions (Alonso et al., 2017). *In situ* calibration in erGAP3-expressing HeLa cells permeabilized with digitonin and treated with a cocktail of ionophores to ensure complete dissipation of the electrochemical gradients gave the same K_d value as the *in vitro* calibration (490±70 µM; mean±s.e.m.). ER-targeted GAP3 expressed in C2C12 myoblasts behaved similarly (Fig. S1). Fig. 1 illustrates the body locations of erGAP3 fluorescence in the transgenic flies generated. The muscle fly line (DM006) expressed the GAP3 probe mainly in the thorax muscle mass (Fig. 1A,B), where it showed good overlap with SERCA (Fig. 1C–E). In the neuronal transgenic fly line (DN005), GAP fluorescence was visible in the brain and in the halteres, as expected from the localization of the pan-neuronal promoter *elav* that drives the expression of erGAP3 (Fig. 1F). Correct performance of the erGAP sensor has been previously shown in several neuron types, both *in vitro* and *ex vivo* (Alonso et al., 2017; Navas-Navarro et al., 2016; Rodriguez-Garcia et al., 2014).

The Ca^{2+} concentration inside the sarcoplasmic reticulum decreases with age

The DM006 flies expressing erGAP3 aged with a median survival time (MST) of 26 days at 29°C, with the females surviving longer than the males (MST, 32 *vs* 19 days, respectively; Fig. S2). In order not to bias the MST estimates, the same numbers of male and female flies were used for all tests. For monitoring muscle function, climbing tests were used, with quantification of both the number of flies that surpassed a threshold (climbing 5 cm) in a certain time (Fig. 2A) and the half-time needed to surpass the threshold (Fig. S3). These climbing tests demonstrated sarcopenia in the flies, which was already significant at day 14 and progressed gradually through the fly lifespan (Fig. 2A; Fig. S3).

The erGAP3 fluorescence ratio of F_{470}/F_{405} is proportional to $[Ca^{2+}]_{ER}$ (Alonso et al., 2017; Navas-Navarro et al., 2016). Therefore, this simple ratiometric measurement in the thoracic muscle mass of the DM006 fly should give quantitative indications of the levels of Ca^{2+} filling in the SR (i.e. $[Ca^{2+}]_{SR}$). The erGAP3

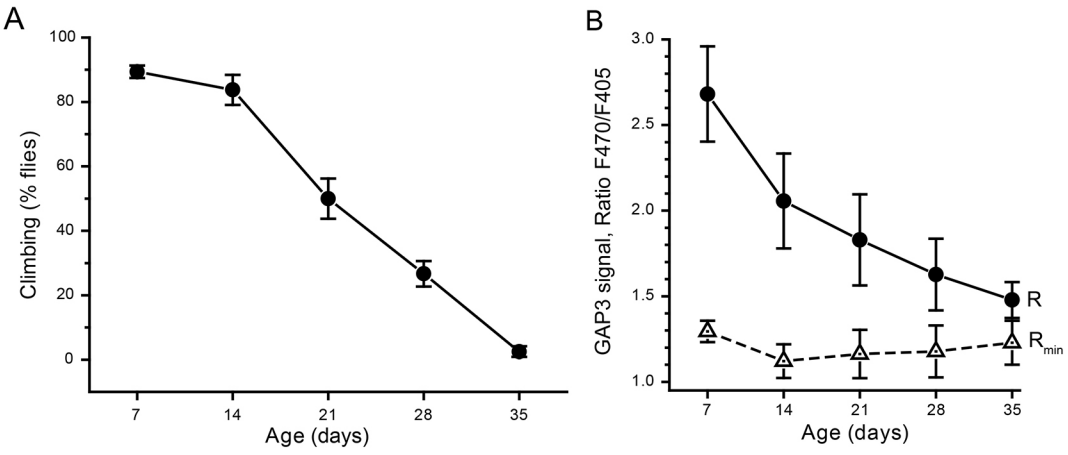

Fig. 2. Comparisons of the climbing efficiency and the F_{470}/F_{405} ratio reached by the muscle erGAP3 in flies of different ages. (A) Climbing assay consisted of counting the number of flies that climbed over 5 cm in height in 18 s. Data are expressed as percentages of the total flies in each group, as means± s.e.m. of 16 flies (same numbers of males and females), except for flies aged 35 days (a group of only eight flies). The linear correlation coefficient of the last four points was 0.997 (P<0.005). (B) Basal erGAP3 fluorescence ratio (R, filled circles) was measured in the thoracic mass of living flies (see Fig. 1B). Data are means± s.d. of 16–20 flies (same numbers of males and females), except for flies aged 35 days (a group of only 10 flies). Triangles, measurements performed in the same flies after 10 min heating at 52°C; these values coincide with the R_{min} values.

Journal of Cell Science (2020) 133, jcs240879. doi:10.1242/jcs.240879

fluorescence ratio was measured for five groups of flies aged 7, 14, 21, 28 and 35 days. As the F_{470}/F_{405} ratio can vary if the experimental settings change, the same settings were maintained for all the measurements (e.g. gain, integration period). The basal F_{470}/F_{405} GAP3 fluorescence ratios are shown in Fig. 2B (R, filled circles). These ratios decreased monotonically with age from 2.68±0.28 (mean±s.d.) in the flies aged 7 days to 1.48±0.10 in the flies aged 35 days. These differences were statistically significant (P<0.0001; One-way ANOVA, Bonferroni multiple comparisons tests).

Calibration of the fluorescence signal and the Ca^{2+} concentrations for *in vivo* measurements

The data shown in Fig. 2B demonstrate the feasibility of this method and the age-dependent decrease in $[Ca^{2+}]_{ER}$, although the calibration of the fluorescent signal into $[Ca^{2+}]$ was not easy, because of the inaccessibility of the Ca^{2+} probe for manipulations during the *in vivo* measurements. In the *in vitro* measurements, this problem was circumvented by ending the measurement protocol with the complete emptying of Ca^{2+} from the ER, to obtain the minimum ratio (R_{min}) for each measurement. Full Ca^{2+} discharge was achieved by perfusion with a Ca^{2+}-releasing agonist in Ca^{2+}-free medium that contained the SERCA inhibitor 2,5-di-*tert*-butylhydroquinone (TBH, 10 µM) (Moore et al., 1990) (Fig. 3A). Knowing that the dynamic range of the GAP3 R_{max}/R_{min} is 3.0, and that the GAP3 K_d is 489 µM, an approximate calibration of the $[Ca^{2+}]$ signals can be performed using the R/R_{min} values (Alonso et al., 2017) according to Eqn 1:

$$R/R_{min} = 1 + (DR - 1) \times ([Ca^{2+}]/(K_d + [Ca^{2+}])), \quad (1)$$

where DR is the dynamic range (R_{max}/R_{min}), $[Ca^{2+}]$ is the Ca^{2+} concentration, and K_d is the Ca^{2+}-GAP3 dissociation constant (479 µM). The resulting R/R_{min} should range between 1.0 at $[Ca^{2+}]$ of 0, and 3.0 at infinite $[Ca^{2+}]$; see Fig. 1B in Alonso et al. (2017). The calibration curve for DR=3.0 and K_d=479 µM is shown in Fig. S4.

During a set of measurements in erGAP3-expressing HeLa cells performed at different temperatures, the F_{470}/F_{405} ratio that was reached after heating the cells for 10 min at 52°C was very similar to the R_{min} estimated using the ER depletion protocol (stimulation with ATP in Ca^{2+}-free medium containing TBH). This finding is illustrated in Fig. 3B, where the cells were initially maximally, but transiently, stimulated with a mixture of inositol 1,4,5-trisphosphate-producing agonists (ATP and carbachol). After the recovery, the ER was completely emptied of Ca^{2+} by applying the same stimulus in Ca^{2+}-free medium containing 10 µM TBH, the SERCA inhibitor. The expected reciprocal changes in the individual fluorescences at F_{470} and F_{405} upon stimulation were recorded (Fig. 3A). The F_{470}/F_{405} ratios are shown in Fig. 3B, for both normal cells ('control') and heated cells ('heated'). The 'heated' value was similar to R_{min}, the value reached after complete Ca^{2+} depletion of the ER (cf. Fig. 3B, control), and it was essentially insensitive to the stimuli.

The data obtained with the different ER-emptying treatments were reproducible, as demonstrated in Fig. 3C, where the mean values (±s.e.m.) of six independent experiments are shown. Note that the height of the 'Heated' bar was not significantly different from the F_{min} bar (ATP+Ca0+TBH). Importantly, the appearance of the HeLa cells under the microscope was not greatly modified by the 52°C heat treatment (Fig. 3D, compare first two panels 'Control' and 'Heated'). Moreover, the changes in fluorescence were similar in the different cells, as demonstrated by the homogeneous intensity of all the pixels in the ratio image (Fig. 3D, right-hand panel). Similar data were obtained in other cell types tested, including HEK293 (human embryonic kidney 293) cells and mouse brain cortical astrocytes, which suggest that a general mechanism is involved (data not shown).

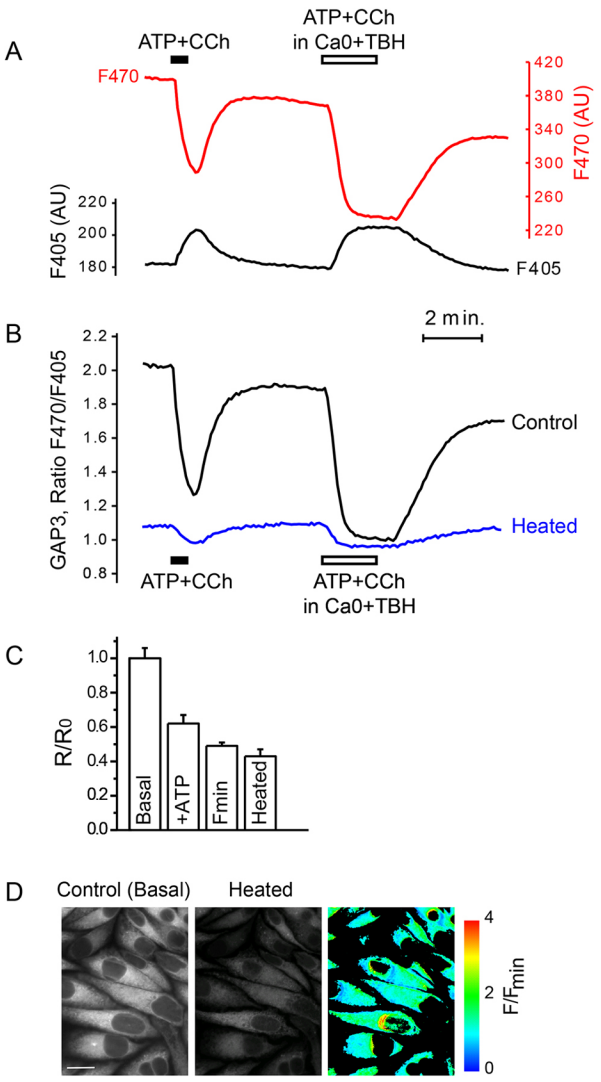

Fig. 3. Calibration of the erGAP3 signal for $[Ca^{2+}]_{ER}$. (A) Partial and complete ER Ca^{2+} emptying by treatment with inositol 1,4,5-trisphosphate-producing agonists [ATP+CCh (carbachol), 100 µM each] in the absence (first challenge) and presence (second challenge) of the SERCA inhibitor TBH, to force full ER emptying. Experiments were performed in the erGAP3 HeLa cell clone. The individual fluorescence, F_{470} (right-hand scale) and F_{405} (left-hand scale) in the control cells are shown. Traces are the average values of 100 cells from the same microscope field. (B) Ratio of the individual fluorescence traces shown in panel A. The data for before ('Control') and after heating at 52°C for 10 min are shown ('Heated'). (C) The ER Ca^{2+} levels expressed as R/R_0, at baseline ('Basal'), after stimulation with inositol 1,4,5-trisphosphate-producing agonists alone ('+ATP'), or together with TBH ('F_{min}'), according to the protocol illustrated in panels A and B, are compared with the value obtained in the heated cells ('Heated'). The means±s.e.m. of six independent experiments are shown. All the conditions showed significantly smaller R/R_0 than baseline (P<0.001; ANOVA, Bonferroni multiple comparisons tests). However, the values of 'F_{min}' and 'Heated' did not differ significantly. (D) erGAP3 fluorescence images taken at 470 nm excitation before ('Control') and after ('Heated') heating under baseline conditions. Scale bar, 10 µm. The right-hand panel shows the pixel-by-pixel ratio of both images (F/F_{min}) coded in pseudocolor (scale on right). Note that the data are very similar among the cells, and also among different ER regions within the same cell.

The observation that heating to 52°C led to erGAP3 fluorescence signals equivalent to the R_{min} values was not expected. The mechanisms can be understood in the light of previous studies

Journal of Cell Science (2020) 133, jcs240879. doi:10.1242/jcs.240879

(Chan et al., 2014). SERCA has been reported to denature at 49°C (Lepock et al., 1990), and therefore Ca^{2+} pumping inside the ER will cease upon heating to 52°C. As a consequence, Ca^{2+} leaks from the ER until the $[Ca^{2+}]$ gradient between the ER and the cytosol has collapsed. Surprisingly, after heating to 52°C, the plasma membrane barrier appears to remain functional enough to preserve a substantial Ca^{2+} electrochemical gradient between the extracellular medium and the cytosol (Chan et al., 2014). Experimental confirmation of such a behavior in erGAP3 HeLa cells is provided in Fig. S5, where the changes in Fluo-4 fluorescence of HeLa cells loaded with this Ca^{2+}-sensitive dye upon stimulation with ATP are compared in control and 52°C-heated cells. In the control cells (Fig. S5Aa), stimulation with ATP increased the Fluo-4 signal (Fig. S5Ab), as expected from the increase in $[Ca^{2+}]_C$ that results from the ATP-induced Ca^{2+} release from the ER. Surprisingly, Fluo-4 was not released from the cells after heating (Fig. S5Ac), although the heated cells did not respond to ATP (cf. Fig. S5Ac,d). Finally, permeabilization of the plasma membrane using digitonin released Fluo-4 from the cells, with a large loss of the green fluorescence (Fig. S5Ae).

Importantly, GAP remained stable and functional after heating to 52°C, as the GAP fusion temperature is 79°C, according to the GAP thermal denaturation assay (Fig. S5B). In addition, the GAP fluorescence spectrum and Ca^{2+} sensitivity (Alonso et al., 2017; Rodriguez-Garcia et al., 2014; Rodríguez-Prados et al., 2015) were preserved at 52°C (Fig. S5C). In summary, heating to 52°C did not dissipate the Ca^{2+} pump-leak steady state of the plasma membrane, but collapsed the ER/cytosol Ca^{2+} gradient, thus allowing measurement of the GAP3 R_{min} and the subsequent $[Ca^{2+}]$ calibration of the dye in living flies. The R_{min} (mean±s.e.m.) estimated by the heating procedure in flies of different ages is shown in Fig. 2B (triangles and dashed lines). These ranged from 1.12 to 1.29, and the individual variation was small.

Normalized sarcoplasmic reticulum $[Ca^{2+}]$ decreases progressively with age and strongly correlates with contractile performance

We next applied this calibration method to measurements obtained in the SR *in vivo*. Thus, the F_{470}/F_{405} ratios (R) obtained in the living flies were normalized by dividing by the R_{min} measured for the same fly after heating to 52°C at the end of the experiment (R/R_{min}). This treatment of the data homogenized the outcomes from different experiments. For example, the coefficients of variation estimated for five sets of flies of different ages were (mean±s.d.; n=5): 11.70 ±3.17% for R, and 8.06±1.54% for R/R_{min}; the difference here was significant (P<0.05; paired t-test). Note that complete Ca^{2+} emptying of the SR would be reflected in a decrease in R/R_{min} to 1.0, whereas according to the estimated dynamic range (Alonso et al., 2017), saturation with Ca^{2+} inside the ER would produce R/R_{min} of 3.0. The $[Ca^{2+}]$ calibration curve used for computations of $[Ca^{2+}]$ is provided in Fig. S5. An approximate Ca^{2+} calibration based on these assumptions is included as the right-hand axis of the R/R_{min} plots of Fig. 4A, which shows the normalized R/R_{min} of five groups of flies of different ages in the 7–35 days age range. There was a gradual and significant decrease in R/R_{min} that reflected the progressive emptying of the SR Ca^{2+} stores with aging. The negative correlation between age and R/R_{min} was significant (r=0.95; P<0.005).

As we also had the information on progression of sarcopenia with age in the same flies (Fig. 2A), it was possible to directly analyze the correlation between $[Ca^{2+}]_{SR}$ and sarcopenia (Fig. 4B). There was close correlation between $[Ca^{2+}]_{SR}$ and muscle contractile function measured in the climbing test. According to the calibration, $[Ca^{2+}]_{SR}$ was ∼600 µM in the young flies (i.e. at 7 days of age). The motor function was maintained while $[Ca^{2+}]_{SR}$ remained >400 µM. However, when $[Ca^{2+}]_{ER}$ dropped below 400 µM, both $[Ca^{2+}]_{SR}$ and the climbing ability decreased with very similar time courses. The oldest flies (i.e. 35 days of age) showed reduced $[Ca^{2+}]_{SR}$ to ∼50 µM, which represented less than one-tenth that of the youngest flies. This large decrease in $[Ca^{2+}]_{SR}$ was associated with an almost total inability for these aged flies to climb. Importantly, the results in the resting $[Ca^{2+}]_{SR}$ were consistent with the cytosolic Ca^{2+} transients measured in flies expressing the cytosolic Ca^{2+} indicator GCaMP (Fig. S6). In these flies, activation of muscle via the giant fiber demonstrated a large reduction of the $[Ca^{2+}]_C$ transients reported by GCaMP in the old flies. These results validate the $[Ca^{2+}]_{SR}$ measurements obtained with GAP3.

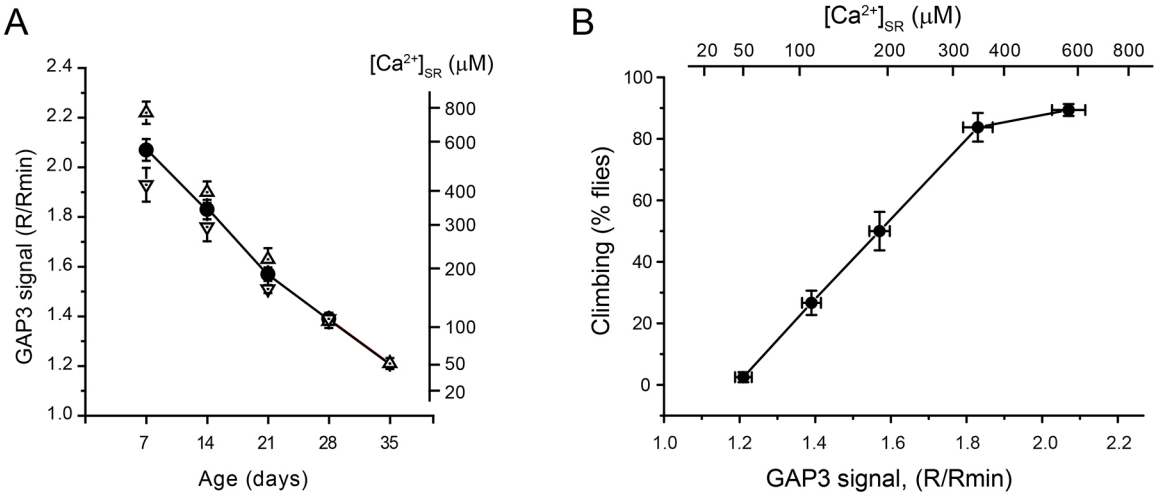

Fig. 4. Decrease in the sarcoplasmic reticulum Ca^{2+} concentration with age, and correlation with climbing ability. (A) The $[Ca^{2+}]_{SR}$ was measured as R/R_{min}. Note that R_{min} corresponds to the completely empty SR. Approximate calibration for $[Ca^{2+}]_{SR}$ as the concentration is given (right-hand scale). Data are means±s.e.m. of 10–20 determinations. Filled circles, all males and females; triangles, females (n=10); inverted triangles, males (n=10). The 35-day-old group contained only 10 female flies and no male flies. All the $[Ca^{2+}]_{SR}$ values were significantly lower than those at 7 days (P<0.001; ANOVA, Bonferroni multiple comparisons tests). (B) Correlation between $[Ca^{2+}]_{SR}$ and fly climbing ability. Note approximate calibration in $[Ca^{2+}]_{SR}$ as concentrations for the upper abscissa axis. Data are means±s.e.m. of groups of 10–20 flies. Other details as in Figs 2A and 4A.

Journal of Cell Science (2020) 133, jcs240879. doi:10.1242/jcs.240879

The expression of SERCA is slightly reduced in the muscle of old flies

The $[Ca^{2+}]_{ER}$ is the result of a pump-leak steady-state condition (Stein, 1967) between SERCA-mediated Ca^{2+} entry and Ca^{2+} leak from the ER. Recent studies have suggested that RyR1 might be the physical substrate of this resting Ca^{2+} leak, especially in aged animals, where oxidative attack on RyR1 and alterations in the RyR1 stabilizing protein Calstabin 1 (also known as FKBP12) can increase the resting conductance of the leak channel (Andersson et al., 2011). To gain insight into the mechanisms responsible for the decrease in $[Ca^{2+}]_{SR}$ during aging, the expression of SERCA and RyR were measured and compared in the young and aged flies.

Fig. 5 summarizes the effects of aging on the expression of three ER proteins: SERCA, the molecular chaperone immunoglobulin-binding protein BIP, and RyR. Total protein expression was normalized to tubulin, and young (7-day-old) and old (35-day-old) flies were compared. BiP and RyR expression were not significantly modified here, whereas expression of SERCA significantly decreased by 35% (P<0.02; ANOVA, Bonferroni multiple comparisons tests). This decrease would tend to decrease $[Ca^{2+}]_{SR}$, although it should be noted that the actual decrease in $[Ca^{2+}]_{SR}$ was much larger (one order of magnitude in Fig. 4).

Endoplasmic reticulum [Ca^{2+}] does not change with age in brain neurons

To investigate if the decrease in $[Ca^{2+}]_{SR}$ in the aged flies was a universal symptom of aging, and was thus also observed in other tissues, the modifications of $[Ca^{2+}]_{ER}$ with age were studied in brain neurons. The transgenic *Drosophila* DN005 line expresses erGAP3 in neurons (Fig. 1F), and this was used here. In contrast to muscle, $[Ca^{2+}]_{ER}$ of the brain neurons did not change significantly with the age of the flies, and remained at ∼400 µM throughout the fly lifetime (Fig. 6). These data indicate that neuronal $[Ca^{2+}]_{ER}$ is less vulnerable than muscle $[Ca^{2+}]_{SR}$ to aging-associated processes.

DISCUSSION

Aging is associated with a decline in physiological functions, which includes loss of muscle mass and strength as one of the most prominent signs (Vijg and Campisi, 2008). Increases in $[Ca^{2+}]_C$ are the trigger for muscle contraction, and therefore a loss of Ca^{2+} homeostasis might be involved in the genesis of sarcopenia. As the increases in $[Ca^{2+}]_C$ are due to the sudden release of Ca^{2+} from the SR, the measurement of $[Ca^{2+}]_{SR}$ is essential to trace the mechanisms of this muscle dysfunction. However, it is difficult to restrict $[Ca^{2+}]$ measurements to just the ER or SR compartments and to avoid contamination by signals from other intracellular compartments. On this basis, we generated a transgenic fly that expressed a genetic Ca^{2+} indicator that was targeted to the ER lumen, erGAP3. In addition, the probe was engineered to have an adequate Ca^{2+} affinity to allow accurate measurements in this high $[Ca^{2+}]$ compartment without saturation (Alonso et al., 2017). The necessity to perform these $[Ca^{2+}]_{SR}$ measurements *in vivo* also made the experimental approach more challenging. To accomplish this task, we developed a novel protocol to calibrate the signal in order to estimate the Ca^{2+} concentrations.

To complicate the issue further, SR Ca^{2+}-binding proteins such as calsequestrin can modify the buffering power in mammalian muscle fibers, thus contributing to shape the SR Ca^{2+} signals (Manno et al., 2017; Ríos, 2018; Sztretye et al., 2011a). The fly muscle SR might show structural and functional features different from mammalian skeletal muscle. For example, the lack of calsequestrin in *Drosophila* is noteworthy. The existence of other

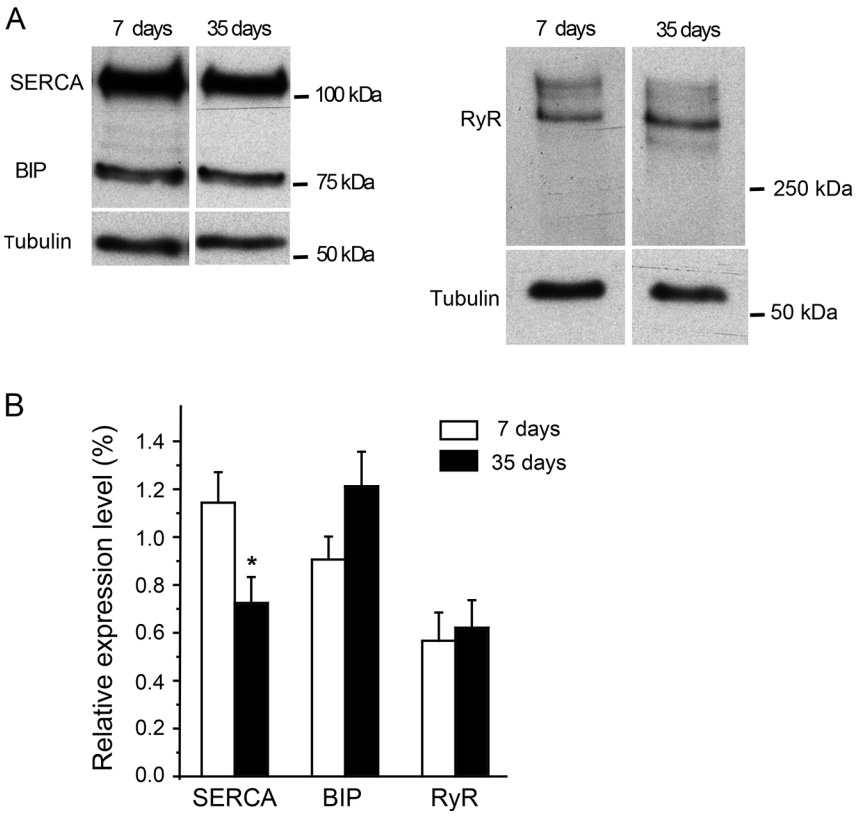

Fig. 5. Comparisons of expression of SERCA, BIP and RyR in young and old flies. (A) Representative data of SERCA, BIP and RyR expression in young (7-day-old) and old (35-day-old) flies. The whole thorax protein extract from one individual fly was loaded per lane, subjected to SDS-PAGE, and revealed with the specific antibodies for SERCA, BIP and RyR. Tubulin was used as the protein loading control. (B) Quantification of multiple data similar to that shown in panel A. They were normalized to the tubulin expression levels, and are means±s.e.m. of 16–32 flies. The reduction in SERCA (35%) was statistically significant (*P<0.02, ANOVA, Bonferroni multiple comparisons tests), whereas differences in expression for the chaperone BIP and for RyR were not statistically significant.

Journal of Cell Science (2020) 133, jcs240879. doi:10.1242/jcs.240879

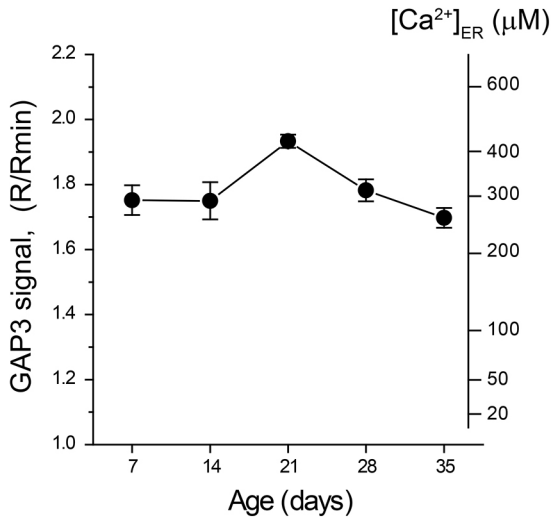

Fig. 6. The endoplasmic reticulum Ca^{2+} concentration of the brain neurons does not change with age. Data were obtained from *elav-erGAP3* flies, and are given as erGAP3 R/R_{min} (left), with approximate calibration in $[Ca^{2+}]_{ER}$ as concentrations on the right. Data are means±s.e.m. of 10–20 determinations in different flies. Variation among the means of the different age groups was not significantly greater than that expected by chance (ANOVA, Bonferroni multiple comparisons tests).

fly SR-resident proteins that might function as calcium buffers cannot be excluded.

We develop here a novel protocol to calibrate the signal in order to estimate Ca^{2+} concentrations. Due to the ratiometric nature of GAP measurements, computation of the Ca^{2+} concentration is feasible if R_{min}, the dynamic range (R_{max}/R_{min}) and K_d are known (Alonso et al., 2017). R_{min} can be easily determined in *in vitro* tests by completely emptying the ER store at the end of each experiment (Fig. 3A; Fig. S1), but this procedure cannot be used in *in vivo* measurements. We found, however, that R_{min} can also be obtained from measurement of the F_{470}/F_{405} ratio in cells heated to 52°C for 10 min (Fig. 3B). The mechanism is not straightforward: the barrier function of the plasma membrane is preserved when heating to 52°C, and $[Ca^{2+}]_C$ remains low. However, heating above 49°C denatures SERCA, so that Ca^{2+}-ATPase activity is impeded (Lepock et al., 1990), and Ca^{2+} is released from the ER into the cytosol. As a result, $[Ca^{2+}]_{ER}$ decreases and the fluorescent signal drops to the R_{min}. This procedure allows normalization of the GAP3 signal and approximate calibration into $[Ca^{2+}]_{ER}$. These data are reproducible from cell to cell, from batch to batch, and among tissues (Fig. 3C).

Our results demonstrate that $[Ca^{2+}]_{SR}$ of the thoracic muscles decreases gradually with age, down to levels as low as one-tenth of those in young flies (Fig. 4A). The correlation with muscle function, which was quantified as the fly climbing ability, revealed near-normal activity at $[Ca^{2+}]_{SR}$ >400 µM, and then a linear decrease in climbing at lower $[Ca^{2+}]_{SR}$ (Fig. 4B). The resting $[Ca^{2+}]_{ER}$ that we measured in different cells (e.g. HeLa, HEK, CHO cells, hippocampal neurons, astrocytes) was from 400 to 700 µM (Rodríguez-Prados et al., 2015), which is in the same range as the values estimated here in the fly skeletal muscle. Our estimates are also consistent with earlier values obtained in mouse muscle fibers (Rudolf et al., 2006; Sztretye et al., 2011b). Therefore, 400 µM appears to be the $[Ca^{2+}]_{SR}$ threshold beneath which muscle function begins to be compromised.

The Ca^{2+} alterations reported in neural tissues have been studied mainly in mouse models, where the focus has been on the loss of Ca^{2+} homeostasis in the cytosol, rather than in the ER (Alzheimer's Association Calcium Hypothesis Workgroup, 2017; Thibault et al., 2007). The different $[Ca^{2+}]_{ER}$ arise from different pump-leak steady-state levels (Stein, 1967), which can be modified by changes either in the expression of SERCA or in the ER Ca^{2+}-leak pathway. Here we provide evidence for a small but significant decrease of SERCA expression (Fig. 5). Although this change might contribute to the drop in $[Ca^{2+}]_{SR}$ in the old flies, the decrease of SERCA appears not to be large enough to explain the large $[Ca^{2+}]_{SR}$ decrease and motor loss observed with increased fly age (Fig. 4). There was also a small, and not significant, increase in RyR expression in aged flies (Fig. 5B), but this cannot explain the observed, much larger $[Ca^{2+}]_{SR}$ decrease, either. We conclude that the increase in the leak must be due to an increase in the resting activity, the leakiness of the leak pathway.

The identity of the ER leak pathway is a controversial matter (Edwards and Kahl, 2010; Ghosh et al., 2017; Lang et al., 2017; Venturi et al., 2013; Yazawa et al., 2007; Zhou et al., 2014; Takeshima et al., 2015). However, recent studies have indicated that in mammalian skeletal muscle, RyR1 might be the physical substrate of an increased leak, especially in aged animals (Andersson et al., 2011; Bellinger et al., 2008; Jiménez-Moreno et al., 2008), where post-translational modifications of RyR1 and/or dissociation of the stabilizing protein Calstabin 1 can increase the resting conductance of the leak channel (Andersson et al., 2011; Mei et al., 2013). A RyR-mediated leakiness that increases with aging has been postulated in muscle for mice (Andersson et al., 2011) and flies (Kreko-Pierce et al., 2016), and even in human B-lymphocytes, where RyR leakiness can be used as a likelihood biomarker for congestive heart failure (Kushnir et al., 2018). This view contrasts with data reported in neural tissues, which have been mainly studied in mouse models, and where loss of Ca^{2+} homeostasis in the cytosolic Ca^{2+} has been frequently proposed (Alzheimer's Association Calcium Hypothesis Workgroup, 2017; Thibault et al., 2007).

It is noteworthy that the $[Ca^{2+}]_{ER}$ collapse with age is not a general event that occurs in every tissue. It was not observed, for example, in brain neurons (Fig. 6). The $[Ca^{2+}]_{ER}$ measured in young brain neurons was lower than that in muscle, but did not vary throughout the fly lifespan. It is tempting to speculate that flies use their skeletal muscle more 'intensively' than their brain neurons, with amplification of the $[Ca^{2+}]_C$ signals by Ca^{2+} release from the ER (i.e. Ca^{2+}-induced Ca^{2+} release). However, amplification of the $[Ca^{2+}]_C$ signal by ER Ca^{2+} release is less frequent in neurons, where the $[Ca^{2+}]_C$ peaks can be predominantly due to Ca^{2+} entry from the extracellular medium rather than to ER Ca^{2+} release. Moreover, the Ca^{2+} channels 'toolkit' in neurons might be very varied, and include plasma membrane and/or endomembrane channels, which can be triggered either by changes in membrane potential or by extracellular or intracellular messengers. In addition, mechanisms for regulation of Ca^{2+} peaks can vary in different regions of the nervous system (He and Jasper, 2014). A further difference between muscle cells and neurons may arise from the presence of cell-specific Ca^{2+}-binding proteins that can shape the Ca^{2+} transients, as demonstrated in mammalian muscle (Manno et al., 2017; Ríos, 2018; Sztretye et al., 2011a).

MATERIALS AND METHODS

Strains and rearing

The *Mhc-erGAP3* fly strain has been reported previously (Navas-Navarro et al., 2016). Here, the Gal4-UAS system (Yao et al., 1993) was used to direct the expression of the ER-targeted GAP3 Ca^{2+} sensor (erGAP3) to

neurons. *UAS-erGAP3* flies (y^1 *w**; M{UAS-erGAP3}ZH-86Fb stored in Bloomington *Drosophila* Stock Center; ref. 80904) were crossed with *elav-Gal4* (embryonic lethal abnormal visual system) flies (Yao et al., 1993), which were a generous gift from Professor Alberto Ferrús (Instituto Cajal, Madrid, Spain). The flies were reared on standard agar medium (Genesee, USA) at 25°C, 60% relative humidity, under a 12 h–12 h light–dark cycle.

Lifespan assay

Curves based on cumulative survival calculations are the most common representation of demographic data (He and Jasper, 2014). Flies were maintained at 29°C. Groups of 20 flies were placed into fresh food vials every 2 or 3 days. Flies that escaped or were dead by accident were immediately excluded from the experiment. The assay lasted until the last survivor died. The data represent the percentages of survival at the day indicated.

Climbing assay

We used two standardized assays to quantify the locomotor behavior excited by negative geotaxis (Gargano et al., 2005; He and Jasper, 2014). In the first assay, each vial containing 10 flies was gently tapped on the table to get the flies to the bottom of the vial, and then left standing for 18 s. The number of flies that climbed more than 5 cm was recorded. In the second assay, we monitored the time in which 50% of the flies passed the 5 cm mark. The flies were left to rest for 15 min, and then the assay was repeated twice. The assays were performed on days 7 (i.e. when the flies were 7 days old), 14, 21, 28 and 35.

Immunohistochemistry

Whole adult flies were embedded and cryopreserved in Tissue-Tek, frozen in dry ice, and stored at −80°C. Cryostat microtome slices (10−15 µm) were fixed in 4% (v/v) paraformaldehyde in phosphate-buffered saline for 30 min, and permeabilized with 0.15% (v/v) Triton X-100 in phosphate-buffered saline containing 5% goat serum. They were then incubated with the anti-SERCA primary antibody (1:500) overnight at 4°C (Sanyal et al., 2006). The samples were washed and revealed with the Alexa Fluor 568-conjugated secondary antibody (1:100; Molecular Probes™ A-11031) at 25°C for 1 h. The samples were mounted on glass slides with Vectashield (Vector Laboratories). GAP was detected as green fluorescence (excited at 470/40 nm, filtered at 540/50 nm) using an imaging microscope (Axioplan 2, Zeiss) equipped with a 63×/1.2w Korr water immersion objective and a camera (AxioCam MR). The red fluorescence was excited at 560/40 and filtered at 605/50 nm. The Zeiss ApoTome system was used for optical sectioning, and the images were analyzed using AxioVision Rel 4.6.3 (Zeiss) and ImageJ (https://imagej.nih.gov/ij/) software.

Ca^{2+} imaging *in vivo*

The flies were anesthetized with CO_2, tethered ventrally in a small drop of warm agar, and then quickly transferred to the stage of a fluorescence stereo microscope (M205FA, Leica). Five fluorescence images of each wavelength were collected at 5 s intervals from either the thoracic muscles or the head neurons. A Plan Apo 1.0× objective (NA=0.35) and a 120 W mercury lamp were used, with either 470/40 or 405/40 nm excitation filters, and a 525/50 nm emission filter. Images were acquired at 16 bits, with binning of 4×4 and a zoom of 6.5×. To determine R_{min} at the end of each measurement, each fly was carefully heated in the bath for 10 min at 52°C, and then imaged using the same settings.

Ca^{2+} imaging *in vitro*

The stably expressing erGAP3 HeLa clone has been previously described (Navas-Navarro et al., 2016). The cells were maintained in Dulbecco's modified Eagle's medium–GlutaMAX (Gibco) supplemented with 100 µg/ml streptomycin and 100 U/ml penicillin, 10% (v/v) fetal bovine serum and 0.2 mg/ml G-418, at 37°C and under 5% CO_2. For imaging experiments, the HeLa cells were seeded onto poly-L-lysine-coated 12 mm diameter glass coverslips at a density of 4×10^4 cells/coverslip. Imaging was performed 1 day later using an upright microscope (Axioplan, Zeiss) equipped with a 20× water-immersion objective (W-Achroplan, Zeiss; NA=0.5) and an AxioCam MRm camera (12 bits; Zeiss). The system was coupled to a xenon lamp with an excitation filter wheel containing the 405/12DF and 470/25DF filters. All experiments were recorded at 22°C. GAP was excited sequentially at 470 and 405 nm, and acquired at >515 nm emission (535DF35 filter), sequentially at each excitation wavelength every 10 s. The system was managed using Zeiss Axiovision software. The background was subtracted from the output images and pixel-to-pixel ratios were calculated using ImageJ software. The ratio R (F_{470}/F_{405}) was used as an index of $[Ca^{2+}]_{ER}$, and was generally expressed as R/R_0 or R/R_{min}. R_0 was computed as the mean of the ratios obtained during the first 5–10 frames of each experiment. The cells were under continuous perfusion (5–6 ml/min) with an 'extracellular-like solution' that contained 145 mM NaCl, 5 mM KCl, 1 mM $CaCl_2$, 1 mM $MgCl_2$, 10 mM glucose and 10 mM Na-HEPES (pH 7.4). The stimuli were dissolved in this extracellular-like medium and perfused for 30 s. For the heating experiments, immediately after the measurements at 25°C, the coverslips were placed in extracellular-like solution at 52°C for 10 min, and then the fluorescence images were captured using the same settings.

Western blotting

The flies were anesthetized with CO_2, and their tissues were dissected and homogenized using a Konte pellet pestle in RIPA buffer (150 mM NaCl, 50 mM Tris-HCl, 0.1% SDS, 0.5% deoxycholate, 1% Triton X-100). Total protein was quantified using the Bradford assay. Whole thorax or head protein from one fly was loaded per lane, subjected to 6% SDS/PAGE, and electrotransferred onto nitrocellulose membranes. These samples were blocked for 2 h with Tris-buffered saline containing 20 mM Tris (pH 7.5), 150 mM NaCl and 0.05% Tween 20 (TBST) plus 2% defatted dried milk. The membranes were then incubated with the primary antibody diluted in blocking solution, overnight at 4°C. The antibody dilutions were as follows: anti-SERCA, 1:10,000 (Sanyal et al., 2006); anti-RyR, 1:2500 (Gao et al., 2013); anti-BIP, 1:5000 (Sigma, G9043); and anti-tubulin, 1:10,000 (Sigma, T6074). After three washes with TBST, the membranes were incubated with the corresponding secondary antibodies labeled with the horseradish peroxidase enzyme (Bio-Rad anti-mouse 170-6516, anti-rabbit 170-6515 or anti-guinea-pig AHP863P) for 1 h at room temperature. After three more washes, the protein was detected by incubation for 1 min with ECL western blotting substrate (Thermo Scientific). The hyperfilms were analyzed by densitometry using ImageJ software. The investigator was blinded to the group allocation during the experiment and during the analysis.

Statistical analysis

Data were analyzed using Origin 7 (OriginLab™) and are expressed as means±s.d. or ±s.e.m., as indicated. The statistical significances were evaluated using one-way ANOVA, with Bonferroni multiple comparisons tests and Student's *t*-test, using GraphPad InStat3 software.

Acknowledgements

The authors would like to thank Jesús Fernández, Miriam García Cubillas and Carla Rodríguez for expert technical help, Dr M. Ramaswami, Trinity College Dublin, Ireland for the anti-SERCA antibody, and Dr R. Scott, NIMH, Bethesda, USA, for the anti-RyR antibody. We acknowledge Dr R. Meijers, EMBL Sample Preparation and Characterization Facility, Hamburg, Germany for GAP thermal denaturation assay.

Competing interests

The authors declare no competing or financial interests.

Author contributions

Conceptualization: M.T.A., J.G.-S.; Methodology: A.D.-L., J.R.-R., M.T.A.; Formal analysis: A.D.-L., J.R.-R., M.T.A., J.G.-S.; Investigation: A.D.-L., J.R.-R., M.T.A., J.G.-S.; Resources: J.G.-S.; Writing - original draft: J.G.-S.; Writing - review & editing: A.D.-L., J.R.-R., M.T.A.; Supervision: J.R.-R., M.T.A., J.G.-S.; Project administration: M.T.A., J.G.-S.; Funding acquisition: M.T.A., J.G.-S.

Funding

This study was supported by grants from the Ministerio de Economía y Competitividad (BFU2017-83066-P) and the Consejería de Educación, Junta de Castilla y León (GR175). J.R.-R. and A.D.-L. were supported by Fellowships from the Spanish Ministerio de Economía y Competitividad.

Supplementary information

Supplementary information available online at
http://jcs.biologists.org/lookup/doi/10.1242/jcs.240879.supplemental

Peer review history

The peer review history is available online at https://jcs.biologists.org/lookup/doi/10.1242/jcs.240879.reviewer-comments.pdf

References

Alonso, M. T., Rojo-Ruiz, J., Navas-Navarro, P., Rodríguez-Prados, M. and García-Sancho, J. (2017). Measuring Ca^{2+} inside intracellular organelles with luminescent and fluorescent aequorin-based sensors. *Biochim. Biophys. Acta Mol. Cell Res.* **1864**, 894-899. doi:10.1016/j.bbamcr.2016.12.003

Allen, D. G., Lamb, G. D. and Westerblad, H. (2008). Skeletal muscle fatigue: cellular mechanisms. *Physiol. Rev.* **88**, 287-332. doi:10.1152/physrev.00015.2007

Alzheimer's Association Calcium Hypothesis Workgroup. (2017). Calcium hypothesis of Alzheimer's disease and brain aging: a framework for integrating new evidence into a comprehensive theory of pathogenesis. *Alzheimers Dement* **13**, 178-182.e17. doi:10.1016/j.jalz.2016.12.006

Andersson, D. C., Betzenhauser, M. J., Reiken, S., Meli, A. C., Umanskaya, A., Xie, W., Shiomi, T., Zalk, R., Lacampagne, A. and Marks, A. R. (2011). Ryanodine receptor oxidation causes intracellular calcium leak and muscle weakness in aging. *Cell Metab.* **14**, 196-207. doi:10.1016/j.cmet.2011.05.014

Bass, T. M., Weinkove, D., Houthoofd, K., Gems, D. and Partridge, L. (2007). Effects of resveratrol on lifespan in *Drosophila melanogaster* and *Caenorhabditis elegans*. *Mech. Ageing Dev.* **128**, 546-552. doi:10.1016/j.mad.2007.07.007

Bellinger, A. M., Reiken, S., Dura, M., Murphy, P. W., Deng, S.-X., Landry, D. W., Nieman, D., Lehnart, S. E., Samaru, M., Lacampagne, A. et al. (2008). Remodeling of ryanodine receptor complex causes 'leaky' channels: a molecular mechanism for decreased exercise capacity. *Proc. Natl. Acad. Sci. USA* **105**, 2198-2202. doi:10.1073/pnas.0711074105

Bellinger, A. M., Reiken, S., Carlson, C., Mongillo, M., Liu, X., Rothman, L., Matecki, S., Lacampagne, A. and Marks, A. R. (2009). Hypernitrosylated ryanodine receptor calcium release channels are leaky in dystrophic muscle. *Nat. Med.* **15**, 325-330. doi:10.1038/nm.1916

Berridge, M. J. (2016). The inositol trisphosphate/calcium signaling pathway in health and disease. *Physiol. Rev.* **96**, 1261-1296. doi:10.1152/physrev.00006.2016

Berridge, M. J., Bootman, M. D. and Roderick, H. L. (2003). Calcium signalling: dynamics, homeostasis and remodelling. *Nat. Rev. Mol. Cell Biol.* **4**, 517-529. doi:10.1038/nrm1155

Canato, M., Scorzeto, M., Giacomello, M., Protasi, F., Reggiani, C. and Stienen, G. J. M. (2010). Massive alterations of sarcoplasmic reticulum free calcium in skeletal muscle fibers lacking calsequestrin revealed by a genetically encoded probe. *Proc. Natl. Acad. Sci. USA* **107**, 22326-22331. doi:10.1073/pnas.1009168108

Chan, C. J., Whyte, G., Boyde, L., Salbreux, G. and Guck, J. (2014). Impact of heating on passive and active biomechanics of suspended cells. *Interface Focus* **4**, 20130069. doi:10.1098/rsfs.2013.0069

Edwards, J. C. and Kahl, C. R. (2010). Chloride channels of intracellular membranes. *FEBS Lett.* **584**, 2102-2111. doi:10.1016/j.febslet.2010.01.037

Efremov, R. G., Leitner, A., Aebersold, R. and Raunser, S. (2015). Architecture and conformational switch mechanism of the ryanodine receptor. *Nature* **517**, 39-43. doi:10.1038/nature13916

Gao, S., Sandstrom, D. J., Smith, H. E., High, B., Marsh, J. W. and Nash, H. A. (2013). *Drosophila* ryanodine receptors mediate general anesthesia by halothane. *Anesthesiology* **118**, 587-601. doi:10.1097/ALN.0b013e31827e52c6

Gargano, J. W., Martin, I., Bhandari, P. and Grotewiel, M. S. (2005). Rapid iterative negative geotaxis (RING): a new method for assessing age-related locomotor decline in *Drosophila*. *Exp. Gerontol.* **40**, 386-395. doi:10.1016/j.exger.2005.02.005

Ghosh, A., Khandelwal, N., Kumar, A. and Bera, A. K. (2017). Leucine-rich repeat-containing 8B protein is associated with the endoplasmic reticulum Ca^{2+} leak in HEK293 cells. *J. Cell Sci.* **130**, 3818-3828. doi:10.1242/jcs.203646

He, Y. and Jasper, H. (2014). Studying aging in *Drosophila*. *Methods* **68**, 129-133. doi:10.1016/j.ymeth.2014.04.008

Jiménez-Moreno, R., Wang, Z.-M., Gerring, R. C. and Delbono, O. (2008). Sarcoplasmic reticulum Ca^{2+} release declines in muscle fibers from aging mice. *Biophys. J.* **94**, 3178-3188. doi:10.1529/biophysj.107.118786

Jiménez-Moreno, R., Wang, Z.-M., Messi, M. L. and Delbono, O. (2010). Sarcoplasmic reticulum Ca^{2+} depletion in adult skeletal muscle fibres measured with the biosensor D1ER. *Pflugers Arch.* **459**, 725-735. doi:10.1007/s00424-009-0778-4

Kabbara, A. A. and Allen, D. G. (2001). The use of the indicator fluo-5N to measure sarcoplasmic reticulum calcium in single muscle fibres of the cane toad. *J. Physiol.* **534**, 87-97. doi:10.1111/j.1469-7793.2001.00087.x

Kreko-Pierce, T., Azpurua, J., Mahoney, R. E. and Eaton, B. A. (2016). Extension of health span and life span in *Drosophila* by S107 requires the calstabin homologue FK506-BP2. *J. Biol. Chem.* **291**, 26045-26055. doi:10.1074/jbc.M116.758839

Kushnir, A., Santulli, G., Reiken, S. R., Coromilas, E., Godfrey, S. J., Brunjes, D. L., Colombo, P. C., Yuzefpolskaya, M., Sokol, S. I., Kitsis, R. N. et al. (2018). Ryanodine receptor calcium leak in circulating B-lymphocytes as a biomarker in heart failure. *Circulation* **138**, 1144-1154. doi:10.1161/CIRCULATIONAHA.117.032703

Lang, S., Pfeffer, S., Lee, P.-H., Cavalié, A., Helms, V., Förster, F. and Zimmermann, R. (2017). An update on Sec61 channel functions, mechanisms, and related diseases. *Front. Physiol.* **8**, 887. doi:10.3389/fphys.2017.00887

Launikonis, B. S., Zhou, J., Royer, L., Shannon, T. R., Brum, G. and Ríos, E. (2005). Confocal imaging of $[Ca^{2+}]$ in cellular organelles by Seer, shifted excitation and emission ratioing of fluorescence. *J. Physiol.* **567**, 523-543. doi:10.1113/jphysiol.2005.087973

Launikonis, B. S., Zhou, J., Royer, L., Shannon, T. R., Brum, G. and Rios, E. (2006). Depletion 'skraps' and dynamic buffering inside the cellular calcium store. *Proc. Natl. Acad. Sci. USA* **103**, 2982-2987. doi:10.1073/pnas.0511252103

Lepock, J. R., Rodahl, A. M., Zhang, C., Heynen, M. L., Waters, B. and Cheng, K. H. (1990). Thermal denaturation of the calcium ATPase of sarcoplasmic reticulum reveals two thermodynamically independent domains. *Biochemistry* **29**, 681-689. doi:10.1021/bi00455a013

Manno, C., Figueroa, L. C., Gillespie, D., Fitts, R., Kang, C. H., Franzini-Armstrong, C. and Rios, E. (2017). Calsequestrin depolymerizes when calcium is depleted in the sarcoplasmic reticulum of working muscle. *Proc. Natl. Acad. Sci. USA* **114**, E638-E647. doi:10.1073/pnas.1620265114

Marzetti, E. and Leeuwenburgh, C. (2006). Skeletal muscle apoptosis, sarcopenia and frailty at old age. *Exp. Gerontol.* **41**, 1234-1238. doi:10.1016/j.exger.2006.08.011

Mei, Y., Xu, L., Kramer, H. F., Tomberlin, G. H., Townsend, C. and Meissner, G. (2013). Stabilization of the skeletal muscle ryanodine receptor ion channel-FKBP12 complex by the 1,4-benzothiazepine derivative S107. *PLoS ONE* **8**, e54208. doi:10.1371/journal.pone.0054208

Moore, G. A., Kass, G. E. N., Duddy, S. K., Farrell, G. C., Llopis, J. and Orrenius, S. (1990). 2,5-Di(tert-butyl)-1,4-benzohydroquinone – a novel mobilizer of the inositol 1,4,5-trisphosphate-sensitive Ca^{2+} pool. *Free Radic. Res. Commun.* **8**, 337-345. doi:10.3109/10715769009053367

Navas-Navarro, P., Rojo-Ruiz, J., Rodriguez-Prados, M., Ganfornina, M. D., Looger, L. L., Alonso, M. T. and García-Sancho, J. (2016). GFP-aequorin protein sensor for *ex vivo* and *in vivo* imaging of Ca^{2+} dynamics in high-Ca^{2+} organelles. *Cell Chem. Biol.* **23**, 738-745. doi:10.1016/j.chembiol.2016.05.010

Ríos, E. (2018). Calcium-induced release of calcium in muscle: 50 years of work and the emerging consensus. *J. Gen. Physiol.* **150**, 521-537. doi:10.1085/jgp.201711959

Rodriguez-Garcia, A., Rojo-Ruiz, J., Navas-Navarro, P., Aulestia, F. J., Gallego-Sandin, S., Garcia-Sancho, J. and Alonso, M. T. (2014). GAP, an aequorin-based fluorescent indicator for imaging Ca^{2+} in organelles. *Proc. Natl. Acad. Sci. USA* **111**, 2584-2589. doi:10.1073/pnas.1316539111

Rodríguez-Prados, M., Rojo-Ruiz, J., Aulestia, F. J., García-Sancho, J. and Alonso, M. T. (2015). A new low-Ca^{2+} affinity GAP indicator to monitor high Ca^{2+} in organelles by luminescence. *Cell Calcium* **58**, 558-564. doi:10.1016/j.ceca.2015.09.002

Rudolf, R., Magalhães, P. J. and Pozzan, T. (2006). Direct *in vivo* monitoring of sarcoplasmic reticulum Ca^{2+} and cytosolic cAMP dynamics in mouse skeletal muscle. *J. Cell Biol.* **173**, 187-193. doi:10.1083/jcb.200601160

Sanyal, S., Jennings, T., Dowse, H. and Ramaswami, M. (2006). Conditional mutations in SERCA, the sarco-endoplasmic reticulum Ca^{2+}-ATPase, alter heart rate and rhythmicity in *Drosophila*. *J. Comp. Physiol. B* **176**, 253-263. doi:10.1007/s00360-005-0046-7

Stein, W. D. (1967). *The Movement of Molecules Across Cell Membranes*. New York and London: Academic Press.

Sztretye, M., Yi, J., Figueroa, L., Zhou, J., Royer, L., Allen, P., Brum, G. and Ríos, E. (2011a). Measurement of RyR permeability reveals a role of calsequestrin in termination of SR Ca^{2+} release in skeletal muscle. *J. Gen. Physiol.* **138**, 231-247. doi:10.1085/jgp.201010592

Sztretye, M., Yi, J., Figueroa, L., Zhou, J., Royer, L. and Ríos, E. (2011b). D4cpv-calsequestrin: a sensitive ratiometric biosensor accurately targeted to the calcium store of skeletal muscle. *J. Gen. Physiol.* **138**, 211-229. doi:10.1085/jgp.201010591

Takeshima, H., Venturi, E. and Sitsapesan, R. (2015). New and notable ion-channels in the sarcoplasmic/endoplasmic reticulum: do they support the process of intracellular Ca^{2+} release? *J. Physiol.* **593**, 3241-3251. doi:10.1113/jphysiol.2014.281881

Thibault, O., Gant, J. C. and Landfield, P. W. (2007). Expansion of the calcium hypothesis of brain aging and Alzheimer's disease: minding the store. *Aging Cell* **6**, 307-317. doi:10.1111/j.1474-9726.2007.00295.x

Venturi, E., Sitsapesan, R., Yamazaki, D. and Takeshima, H. (2013). TRIC channels supporting efficient Ca^{2+} release from intracellular stores. *Pflugers Arch.* **465**, 187-195. doi:10.1007/s00424-012-1197-5

Vijg, J. and Campisi, J. (2008). Puzzles, promises and a cure for ageing. *Nature* **454**, 1065-1071. doi:10.1038/nature07216

Yao, K.-M., Samson, M.-L., Reeves, R. and White, K. (1993). Gene *elav* of *Drosophila melanogaster*: a prototype for neuronal-specific RNA binding protein

gene family that is conserved in flies and humans. *J. Neurobiol.* **24**, 723-739. doi:10.1002/neu.480240604

Yazawa, M., Ferrante, C., Feng, J., Mio, K., Ogura, T., Zhang, M., Lin, P.-H., Pan, Z., Komazaki, S., Kato, K. et al. (2007). TRIC channels are essential for Ca^{2+} handling in intracellular stores. *Nature* **448**, 78-82. doi:10.1038/nature05928

Zalk, R., Lehnart, S. E. and Marks, A. R. (2007). Modulation of the ryanodine receptor and intracellular calcium. *Annu. Rev. Biochem.* **76**, 367-385. doi:10.1146/annurev.biochem.76.053105.094237

Zhou, X., Lin, P., Yamazaki, D., Park, K. H., Komazaki, S., Chen, S. R. W., Takeshima, H. and Ma, J. (2014). Trimeric intracellular cation channels and sarcoplasmic/endoplasmic reticulum calcium homeostasis. *Circ. Res.* **114**, 706-716. doi:10.1161/CIRCRESAHA.114.301816

Ziman, A. P., Ward, C. W., Rodney, G. G., Lederer, W. J. and Bloch, R. J. (2010). Quantitative measurement of Ca^{2+} in the sarcoplasmic reticulum lumen of mammalian skeletal muscle. *Biophys. J.* **99**, 2705-2714. doi:10.1016/j.bpj.2010.08.032